

3-19-2013

Marked improvement of cytotoxic effects induced by docetaxel on highly metastatic and androgen-independent prostate cancer cells by downregulating macrophage inhibitory cytokine-1.

M Mimeault
University of Nebraska Medical Center

Sonny L. Johansson
University of Nebraska Medical Center, sjohanss@unmc.edu

Surinder K. Batra
University of Nebraska Medical Center, sbatra@unmc.edu

Follow this and additional works at: https://digitalcommons.unmc.edu/com_bio_articles

 Part of the [Medical Biochemistry Commons](#), and the [Medical Molecular Biology Commons](#)

Recommended Citation

Mimeault, M; Johansson, Sonny L.; and Batra, Surinder K., "Marked improvement of cytotoxic effects induced by docetaxel on highly metastatic and androgen-independent prostate cancer cells by downregulating macrophage inhibitory cytokine-1." (2013). *Journal Articles: Biochemistry & Molecular Biology*. 78.

https://digitalcommons.unmc.edu/com_bio_articles/78

This Article is brought to you for free and open access by the Biochemistry & Molecular Biology at DigitalCommons@UNMC. It has been accepted for inclusion in Journal Articles: Biochemistry & Molecular Biology by an authorized administrator of DigitalCommons@UNMC. For more information, please contact digitalcommons@unmc.edu.

Keywords: macrophage inhibitory cytokine-1; prostate cancer; metastases; chemoresistance; docetaxel; targeted therapy

Marked improvement of cytotoxic effects induced by docetaxel on highly metastatic and androgen-independent prostate cancer cells by downregulating macrophage inhibitory cytokine-1

M Mimeault^{*1}, S L Johansson² and S K Batra^{*1,2}

¹Department of Biochemistry and Molecular Biology, College of Medicine, Eppley Cancer Center, University of Nebraska Medical Center, Omaha, NE 68198-5870, USA and ²Department of Pathology and Microbiology, College of Medicine, Eppley Cancer Center, University of Nebraska Medical Center, Omaha, NE 68198-5870, USA

Background: Overexpression of macrophage inhibitory cytokine-1 (MIC-1) frequently occurs during the progression of prostate cancer (PC) to androgen-independent (AI) and metastatic disease states and is associated with a poor outcome of patients.

Methods: The gain- and loss-of-function analyses of MIC-1 were performed to establish its implications for aggressive and chemoresistant phenotypes of metastatic and AI PC cells and the benefit of its downregulation for reversing docetaxel resistance.

Results: The results have indicated that an enhanced level of secreted MIC-1 protein in PC3 cells is associated with their acquisition of epithelial–mesenchymal transition features and higher invasive capacity and docetaxel resistance. Importantly, the downregulation of MIC-1 in LNCaP-LN3 and PC3M-LN4 cells significantly decreased their invasive capacity and promoted the antiproliferative, anti-invasive and mitochondrial- and caspase-dependent apoptotic effects induced by docetaxel. The downregulation of MIC-1 in PC3M-LN4 cells was also effective in promoting the cytotoxic effects induced by docetaxel on the side population (SP) endowed with stem cell-like properties and the non-SP cell fraction from PC3M-LN4 cells.

Conclusion: These data suggest that the downregulation of MIC-1 may constitute a potential therapeutic strategy for improving the efficacy of current docetaxel-based chemotherapies, eradicating the total mass of PC cells and thereby preventing disease relapse and the death of PC patients.

Human macrophage inhibitory cytokine-1 (MIC-1), also known as growth and differentiation factor-15 (GDF-15), is a divergent member of the transforming growth factor- β (TGF- β)/bone morphogenic protein superfamily (Mimeault and Batra, 2010a). The MIC-1 plays key physiological roles during the prenatal development and regulation of growth and differentiation, cartilage and bone formation, cellular responses to stress and inflammation and tissue repair after acute injuries in postnatal and adult life

(Mimeault and Batra, 2010a). The MIC-1 protein has attracted much attention following the demonstration that it is over-expressed during the progression of numerous aggressive and recurrent cancers, including prostate cancer (PC), and represents a determinant factor associated with tumour growth, metastases, treatment resistance and poor outcome of cancer patients (Lee *et al*, 2003; Liu *et al*, 2003; Nakamura *et al*, 2003; Welsh *et al*, 2003; Cheung *et al*, 2004; Bauskin *et al*, 2005; Wollmann *et al*, 2005;

*Correspondence: Dr M Mimeault; E-mail: mmimeault@unmc.edu or Dr SK Batra; E-mail: sbatra@unmc.edu

Received 30 July 2012; revised 3 October 2012; accepted 3 October 2012; published online 28 February 2013

© 2013 Cancer Research UK. All rights reserved 0007–0920/13

Brown *et al*, 2006; Chen *et al*, 2007; Huang *et al*, 2007; Kim *et al*, 2008; Boyle *et al*, 2009; Zhang *et al*, 2009; Huh *et al*, 2010; Mimeault and Batra, 2010a; Senapati *et al*, 2010). More recently, the serum level of MIC-1 has also been proposed as a new potential marker of all-cause mortality and/or predictor of disease progression, including for various cancers, cardiovascular diseases, chronic renal failure and pulmonary emboli (Wiklund *et al*, 2010).

Although the MIC-1 receptors have not been precisely identified, it has been reported that the secreted MIC-1 protein can induce its biological effects through the activation of type I and type II membrane serine/threonine kinase receptors for TGF- β family members (Tan *et al*, 2000; Xu *et al*, 2006; Johnen *et al*, 2007; Soto-Cerrato *et al*, 2007; Ago *et al*, 2010; Mimeault and Batra, 2010a). In fact, in analogy with TGF- β family ligands, MIC-1 can display dual functions, by inducing growth arrest and differentiation in normal epithelial cells while promoting proliferation, invasion and metastases of PC cells (Lee *et al*, 2003; Wollmann *et al*, 2005; Chen *et al*, 2007; Noorali *et al*, 2007; Kim *et al*, 2008; Boyle *et al*, 2009; Huh *et al*, 2010; Mimeault and Batra, 2010a; Senapati *et al*, 2010; Mimeault *et al*, 2012). This is likely because of the alterations in signal transduction mechanisms mediating the anticarcinogenic effects of MIC-1 in cancer cells and its immunosuppressive effects (Lee *et al*, 2003; Wollmann *et al*, 2005; Chen *et al*, 2007; Noorali *et al*, 2007; Kim *et al*, 2008; Boyle *et al*, 2009; Huh *et al*, 2010; Mimeault and Batra, 2010a, b; Senapati *et al*, 2010). Moreover, it has been reported that the oncogenic effects induced by the secreted MIC-1 protein may be mediated in part through the activation of epidermal growth factor receptor (EGFR) family members, mitogen-activated protein kinases (MAPKs), phosphatidylinositol 3'-kinase/Akt, focal adhesion kinase (FAK) and/or urokinase-type plasminogen activator system in a cancer cell type- and context-dependent manner as well as via the induction of the angiogenic process (Lee *et al*, 2003; Wollmann *et al*, 2005; Chen *et al*, 2007; Kim *et al*, 2008; Boyle *et al*, 2009; Huh *et al*, 2010; Mimeault and Batra, 2010a; Senapati *et al*, 2010; Mimeault *et al*, 2012).

A progressive increase of MIC-1 levels in PC cells and serum samples has also been observed during PC progression to androgen-independent (AI) and metastatic disease states and associated with treatment resistance and a poor prognosis for PC patients (Karan *et al*, 2002; Welsh *et al*, 2003; Zheng *et al*, 2003; Cheung *et al*, 2004; Bauskin *et al*, 2005; Brown *et al*, 2006; Chen *et al*, 2007; Huang *et al*, 2007; Patrikainen *et al*, 2007; Selander *et al*, 2007; Wakchoure *et al*, 2009; Zhao *et al*, 2009; Mimeault and Batra, 2010a; Senapati *et al*, 2010; Mimeault *et al*, 2012). The results from our recent work, and prior studies, have also indicated a functional role of MIC-1 for the sustained growth, reduced intercellular adhesion and enhanced invasive and metastatic properties of PC cells (Liu *et al*, 2003; Chen *et al*, 2007; Huang *et al*, 2007; Patrikainen *et al*, 2007; Zhao *et al*, 2009; Mimeault and Batra, 2010a; Senapati *et al*, 2010; Mimeault *et al*, 2012). In addition, the overexpression of MIC-1 in PC cells has also been linked with the formation of bone metastases and osteoblastic/lytic lesions, which are associated with severe pain in PC patients as well as tumour-induced anorexia and weight loss in late-stage disease (Chen *et al*, 2007; Johnen *et al*, 2007; Wakchoure *et al*, 2009; Zhao *et al*, 2009; Senapati *et al*, 2010).

Additional studies are still necessary to more precisely define the molecular mechanisms of MIC-1 functions for the acquisition of a more malignant behaviour and chemoresistant phenotypes by PC cells during disease progression to metastatic castration-resistant prostate cancers (CRPCs) and the therapeutic interest of its downregulation for reversing chemoresistance. Therefore, gain- and loss-of-function studies were undertaken to establish the MIC-1 implication in the resistance of metastatic and AI PC cells to the cytotoxic effects induced by current chemotherapeutic drug, docetaxel, which is used for treating patients with locally advanced

and metastatic CRPCs. Overall, the results have indicated therapeutic benefits of downregulating the MIC-1 protein to improve the anticarcinogenic effects induced by docetaxel on metastatic and AI PC cells, including CD133⁺ and CD133⁻ PC cell fractions, and eradicate the total mass of PC cells.

MATERIALS AND METHODS

Materials and cell cultures. The human metastatic and AI PC3 cell line was originally purchased from American Type Culture Collection (ATCC, Manassas, VA, USA) and authenticated by short tandem repeat analysis. PC3 cells were used at <20 passages after purchase from ATCC. The well-characterised and highly metastatic and AI LNCaP-LN3 and PC3M-LN4 cell variants of parental LNCaP and PC3 cells, respectively, were established and kindly provided by Dr Isaak J Fidler (University of Texas MD Anderson Cancer Center, Houston, TX, USA) (Pettaway *et al*, 1996). A pooled population of stable clones of MIC-1-transfected PC3 cells overexpressing functional MIC-1 protein (PC3-MIC-1) and empty-vector (pMSCV.puro)-transfected PC3 cell lines (PC3-Vec) was established in our laboratory as previously described (Senapati *et al*, 2010). The LNCaP-LN3-siMIC-1 and PC3M-LN4-siMIC-1 cells in which MIC-1 was downregulated by stealth RNAi-mediated approach as well as LNCaP-LN3-Con and PC3M-LN4-Con cells transfected with control siRNA oligos and expressing high endogenous level of MIC-1 used as a control were prepared as previously described (Senapati *et al*, 2010). All PC cells and their derivative cell lines were maintained as recommended by ATCC guidelines in regular phenol red-free RPMI-1640 culture medium (Gibco, Grand Island, NY, USA) supplemented with 10% fetal bovine serum (FBS), 1% glutamine and 1% penicillin-streptomycin in a 37 °C incubator supplied with 5% CO₂ and routinely tested for morphological features and mycoplasmas (Roche Diagnostics, Indianapolis, IN, USA).

All culture materials were purchased from Life Technologies (Carlsbad, CA, USA) and human recombinant MIC-1 protein (rhMIC-1) was obtained from R&D Systems (Minneapolis, MN, USA). In addition, SB431542, docetaxel, 3',3'-dihydroxycarbocyanine iodide (DiOC₆(3)), (3-(4,5-dimethylthiazol-2-yl)-2,5-diphenyltetrazolium bromide (MTT) and EGF were purchased from Sigma-Aldrich (St Louis, MO, USA) and *N*-benzyloxycarbonyl-Val-Ala-Asp-fluoromethylketone (Z-VAD-FMK) from Calbiochem Corp. (San Diego, CA, USA). The mouse monoclonal anti-vimentin (V6630) and anti- β -actin (clone AC-15) antibodies were purchased from Sigma-Aldrich and mouse anti-E-cadherin and anti-N-cadherin were obtained from BD Biosciences (Franklin Lakes, NJ, USA). The rabbit polyclonal anti-CD133 antibody (H-284) and anti-ABCG2 antibody (B-25), mouse monoclonal anti-CD44 (HCAM, F-4) antibody and anti-cytochrome *c* (6H2) antibody were provided by Santa Cruz Biotechnology, Inc. (Santa Cruz, CA, USA). The rabbit polyclonal anti-MIC-1 antibody was generated in our laboratory as previously described (Chen *et al*, 2007). Moreover, rabbit polyclonal antibody directed against the cleaved fragment of caspase-9 or caspase-3 was purchased from Cell Signaling Technology (Danvers, MA, USA), and rabbit polyclonal antibody recognising the cleaved human poly (ADP-ribose) polymerase (PARP; 197–214) fragment was obtained from Calbiochem, Inc. (San Diego, CA, USA). The phycoerythrin-conjugated monoclonal anti-CD133/2 antibody (293C3) was purchased from Miltenyi Biotec Inc. (Auburn, CA, USA) and employed according to the manufacturer's instructions.

Immunohistochemical analyses. Immunohistochemical studies on the expression of the MIC-1 protein in nonmalignant and malignant prostate tissues were done as previously described by a peroxidase method using the VECTASTAIN avidin-biotin

complex (ABC) kit as indicated in manufacturer's instructions from Vector Laboratories (Burlingame, CA, USA) (Mimeault *et al*, 2007a, b, 2010a, b, 2012). Immunostaining was carried out on AccuMax array tissue sections (Petagen, Inc., Shinchon-dong, Seoul, Korea) containing 8 normal prostatic tissue specimens of biopsy as well as AccuMax array containing 32 pairs of tissue sections from patients with primary prostatic adenocarcinoma (Gleason scores 7–9) with their corresponding adjacent benign tissues from the same patients. A reddish brown colour precipitate observed on tissue sections is indicative of a positive immunoreactivity with the tested primary antibody. For each tissue section, the intensity of immunoreactivity for the MIC-1 protein was semiquantitatively graded by a urological pathologist (SLJ) on a 0 to +3 scale (0 = no staining, 1+ = weak staining, 2+ = moderately strong and 3+ = strong staining). The percentage of PC cells positive for MIC-1 staining within a given tissue core was also scored on a 1 to 4 scale (1 = 0–25% positive PC cells, 2 = 26–50% positive cells, 3 = 51–75% positive cells and 4 = 76–100% positive cells). The score of the staining intensity and the percentage of immunoreactive PC cells were then multiplied to obtain a composite score ranging from 0 to 12. The staining intensity of MIC-1 protein in prostate adenocarcinoma samples was scored and compared with normal and adjacent benign prostatic tissues, and the value was considered enhanced if the staining intensity was higher by one or more points.

Immunoblot and immunofluorescence analyses. The samples of PC cell lysates, conditioned medium or cytosolic fraction corresponding to 20 μ g proteins were resolved by electrophoresis on an 8% or 10% SDS-agarose gel under reducing conditions as previously described (Mimeault *et al*, 2006, 2007a, b, 2010b, 2012). The proteins were transferred onto an immobilon-P transfer membrane and blocked in 5% non-fat dry milk in PBS for 2 h and subjected to the standard immunodetection procedure. At the end of incubation, the blot was washed in TBST (50 mM Tris-HCl, pH 7.4, 150 mM NaCl and 0.05% Tween) and incubated with horseradish peroxidase-conjugated secondary antibody (Amersham Biosciences, Piscataway, NJ, USA) for 1 h. Antibody-antigen complexes were visualised using enhanced chemiluminescence kit (Amersham Biosciences).

Confocal immunofluorescence microscopy. Prostate cancer cells were grown at a low density on sterilised cover slips for 24 h. After washing with PBS, cells were fixed in ice-cold methanol at -20°C for 2 min (Mimeault *et al*, 2007a, b, 2010a, b, 2012). For phalloidin staining, PC cells were fixed in 3.7% formaldehyde-PBS solution for 10 min at room temperature, washed twice with PBS and permeabilised with 0.1% Triton X-100 in PBS for 3–5 min at room temperature. After washing with PBS, nonspecific blocking was carried out using 10% goat serum for 30 min. After the blocking step and a quick wash in PBS, cells were incubated with an antibody directed against E-cadherin, N-cadherin, vimentin, β -actin, ABCG2, CD44, MIC-1 or EGFR/Tyr¹¹⁷³-pEGFR for 1 h at room temperature. After three washes with PBS, the cells were then incubated with fluorescein isothiocyanate (FITC)-conjugated goat anti-mouse, FITC-conjugated donkey anti-goat and/or Texas red-conjugated goat anti-rabbit secondary antibody (Jackson ImmunoResearch Laboratories, Inc., West Grove, PA, USA) for 1 h. For F-actin staining, cells were incubated with rhodamine phalloidin (R415; Molecular Probes, Eugene, OR, USA) for 20 min at room temperature. Cells were washed again three times with PBS, nuclei counterstained with diaminidino-2-phenylindole (DAPI) and mounted on glass slides in anti-fade Vestashield mounting medium (Vector Laboratories). The stained cells were observed under a confocal laser-scanning microscope (LSM 410, Zeiss, Gottingen, Germany) and photographs were taken digitally using LSM 510 software.

Cell growth and flow cytofluorimetric analyses. For growth assays, PC cells were seeded on 96-well plates at a density of 3×10^4 cells per well in a culture medium containing 0.5% FBS and untreated or treated with 2–10 nM docetaxel (Mimeault *et al*, 2006, 2007a, b, 2010a, b, 2012). After incubation for 48 h, the rate of cell growth was estimated by a MTT colorimetric test. For flow cytofluorimetric analyses, all tested PC cells were grown at a density of 5×10^5 cells on 25 cm² dishes. Fluorescence-activated cell sorting (FACS) analyses of cell populations in cell cycle phases were performed after 48-h incubation of PC cells with 2–10 nM docetaxel (Mimeault *et al*, 2005, 2006, 2007a, b, 2010a, b, 2012). The cells were untreated or treated with 2–10 nM docetaxel in the absence or presence of broad caspase inhibitor Z-VAD-FMK at 50 μ M for 4 days. The apoptotic effect induced by docetaxel on PC cells was estimated by FACS analyses by staining of each sample with the propidium iodide as previously described (Mimeault *et al*, 2005, 2006, 2007a, b, 2010a, b, 2012).

In vitro invasion assays. Parental PC3 cells were untreated (control) or pretreated with 1 ng ml⁻¹ rhMIC-1 protein in the presence or absence of 10 μ M SB431542, which is a selective and potent inhibitor of the TGF- β superfamily type I activin receptor-like kinase (ALK) receptor, including ALK4, ALK5 and ALK7, or 10 nM docetaxel for 24 h, and during cell invasion assay for an additional 24 h. Moreover, PC3-Vect vs PC3-MIC-1 cells as well as LNCaP-LN3-Con vs LNCaP-LN3-siMIC-1 and PC3M-LN4-Con vs PC3M-LN4-siMIC-1 cells were untreated (control) or pretreated with 10 nM docetaxel for 24 h, and during cell invasion assay for an additional 24 h. For each experiment, 3×10^5 PC cells per well in a total volume of 2 ml serum-free medium without rhMIC-1 and docetaxel (control) or containing 1 ng ml⁻¹ rhMIC-1 and/or 10 nM docetaxel were loaded into the top of the BioCoat matrigel cell invasion chamber (BD Biosciences, Bedford, MA, USA). The bottom chamber of the well was filled with 2.0 ml of 10% serum-containing medium as a chemoattractant solution and the cells were allowed to migrate for 24 h at 37 $^{\circ}\text{C}$ under chemotactic drive. At the end of incubation, the invasive cells reaching the lower chamber were stained with a Diff-Quick stain set (Dade Behring Inc., Newark, DE, USA) and counted in different fields at a magnification of $\times 100$ using a haemocytometer by phase-contrast microscopy. The results are presented as the average number of invasive cells per representative field.

Estimation of mitochondrial membrane potential (MMP), caspase activation and DNA fragmentation. PC3M-LN4-Con and PC3M-LN4-siMIC-1 cells were untreated (control) or treated with 10 nM docetaxel for 4 days. The adherent and floating cells were collected, rinsed twice with PBS and centrifuged. For the MMP estimation, the pellets corresponding to $\sim 1 \times 10^6$ PC cells were resuspended in 1 ml PBS containing the cationic, lipophilic and fluorescent dye, 40 nM DiOC₆(3), which specifically accumulates within the mitochondrial compartment in a MMP-dependent manner. After incubation at 37 $^{\circ}\text{C}$ for 20 min, the accumulation of DiOC₆(3) within the mitochondria of PC cells was measured by FACS analyses. Moreover, the amounts of cytochrome *c* present in the cytosolic extracts and cleaved caspase-9 or caspase-3 fragment and cleaved PARP fragment in each sample were estimated by western blot analyses as described above.

In addition, the qualitative analysis of DNA fragmentation associated with the apoptotic death of PC3M-LN4-Con and PC3M-LN4-siMIC-1 cells induced by docetaxel was performed by the electrophoretic method (Mimeault *et al*, 2006). Briefly, PC cells were grown for 4 days without docetaxel (control) or treated with 10 nM docetaxel. The adherent and floating PC cells were collected by centrifugation, and DNA from each sample was extracted using Gentra's Puregene DNA Isolation Kit (Qiagen, Valencia, CA, USA) protocol and analysed on a 0.8% agarose gel electrophoresis. The gel was visualised on UV light after

staining with ethidium bromide, and the DNA patterns were photographed.

Isolation and characterisation of the phenotypic and functional features of SP and non-SP PC3M-LN4 cell fractions. The PC3M-LN4 cells (1×10^6 cells per ml) were stained with $2 \mu\text{g ml}^{-1}$ fluorescent Hoechst dye at 37°C for 2 h in the absence or presence of $50 \mu\text{M}$ verapamil as previously described (Mimeault and Batra, 2009; Mimeault *et al.*, 2010a,b, 2012). The analyses and sorting of the viable side population (SP) and non-SP cell fractions were done using a FACS Aria flow cytometer with a DIVA software (Becton Dickinson Biosciences, San Jose, CA, USA). The monolayer clonogenic and prostasphere-forming assays were then performed to estimate the self-renewal capacity of SP vs non-SP PC3M-LN4 cell fractions (Mimeault *et al.*, 2012). Briefly, for each clonogenic assay, 500 viable SP or non-SP PC3M-LN4 cells were suspended in serum-free medium supplemented with 1% L-glutamine, antibiotics and EGF (10 ng ml^{-1}) onto a 120-mm dish. All samples were plated in triplicate. After 14 days, the cultures were fixed and directly stained with a crystal violet solution and colonies were counted. For prostasphere-forming assay, 500 viable SP or non-SP PC3M-LN4 cells were suspended in serum-free medium onto a six-well ultra-low attachment plate (Corning, Invitrogen, Inc., Denver, CO, USA). All samples were plated in triplicate. After 7 days of incubation, the number of SP PC3M-LN4 cell-derived prostaspheres was counted and representative pictures of prostaspheres were photographed by using Accu-scope phase-contrast microscope at a magnification of $\times 200$. In addition, PC3M-LN4-Con and PC3M-LN4-siMIC-1 cells (1×10^6 cells per ml) were stained with fluorescent Hoechst dye at 37°C for 2 h in the absence or presence of 10 nM docetaxel. The viability of SP and non-SP cells was analysed by FACS as previously described (Mimeault and Batra, 2009; Mimeault *et al.*, 2010a, b, 2012).

Statistical analyses. Statistical analyses were performed using the Student's *t*-test to compare the results, with *P*-values < 0.05 indicating statistically significant differences. More specifically, immunohistochemical data were analysed using MedCalc for Windows version 9.6.4.0. software (MedCalc Software, Mariakerke, Belgium). The composite scores of MIC-1 expression were considered as continuous variables and compared using Student's two-tailed *t*-test assuming unequal variance for independent samples.

RESULTS

Immunohistochemical analyses of MIC-1 expression level in malignant prostate tissues vs nonmalignant adjacent prostate tissues. The results from immunohistochemical analyses have revealed that MIC-1 was overexpressed in 84% of prostatic adenocarcinomas analysed as compared with normal prostatic tissues of biopsy (mean of composite scores: 3.9 ± 0.4 vs 0.4 ± 0.3 ; $P \leq 0.0001$), respectively (Figures 1A and B and Table 1). Moreover, the expression level of MIC-1 was also enhanced in 72% of prostatic adenocarcinomas analysed relative to their corresponding adjacent benign tissues from 32 PC patients (Gleason scores = 7–9; mean of composite scores: 3.9 ± 0.4 vs 1.5 ± 0.3 ; $P \leq 0.0001$), respectively (Figures 1A and B and Table 1). Moreover, the MIC-1 expression in adjacent nonmalignant prostatic tissue specimens was significantly enhanced in 59% (1.5 ± 0.3) cases as compared with normal prostatic tissues (0.4 ± 0.3 ; $P < 0.005$; Figure 1B and Table 1). More particularly, MIC-1 was weakly expressed in basal and luminal epithelial cells in normal and adjacent benign prostatic tissues, whereas a higher expression of MIC-1 was detected in the cytoplasm as well as at or near the cell surface in luminal and intermediate tumour cells in malignant prostatic tissues (Figure 1A). Furthermore, the staining intensity of the secreted MIC-1 protein detected in the stromal

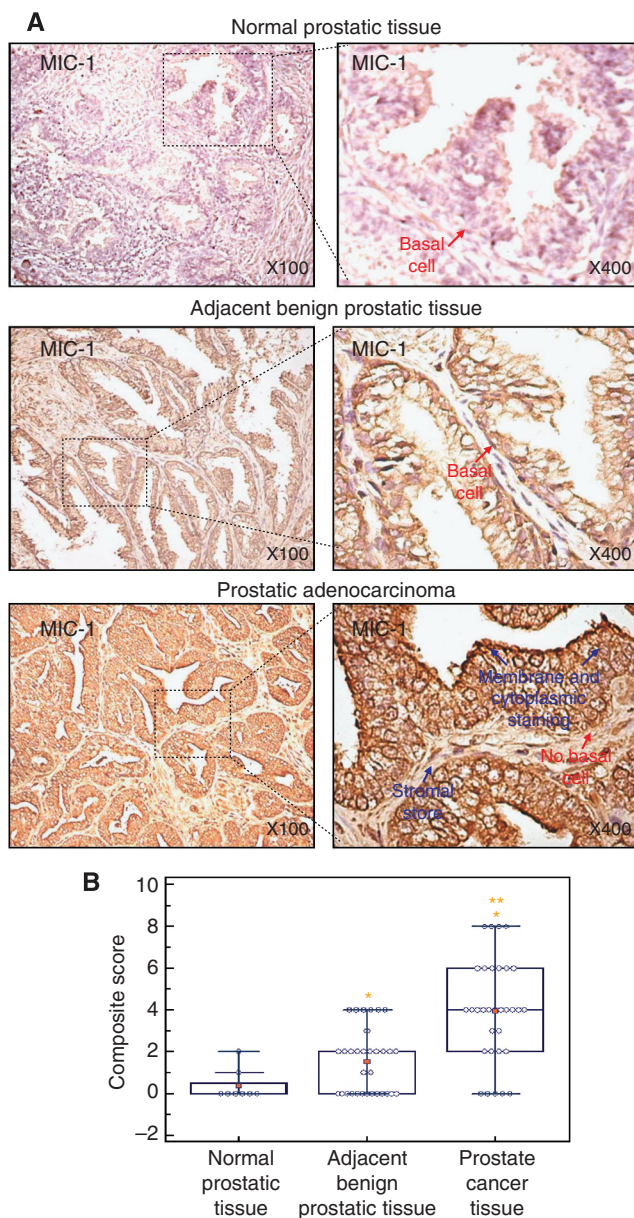


Figure 1. Immunohistochemical analyses of expression levels of the MIC-1 protein in nonmalignant and malignant prostatic tissues. (A) Representative pictures of immunohistochemical analyses of the expression level of MIC-1 in normal prostatic tissues from biopsies and adjacent benign and prostatic adenocarcinoma tissues from same PC patients are shown at original magnifications of $\times 100$ and $\times 400$. (B) Comparison of the composite scores of expression levels of MIC-1 in nonmalignant and malignant tissues from PC patients. Box plots showing the expression levels of MIC-1 in normal prostatic tissues from biopsies and prostatic adenocarcinoma specimens and their adjacent benign prostatic tissues. * $P < 0.005$ and 0.0001 indicates a significant increase between the means of composite scores obtained for adjacent benign prostatic tissues and prostatic adenocarcinoma tissues relative to mean of composite scores obtained for normal prostatic tissue specimens. ** $P < 0.0001$ indicates a significant increase between the mean of composite scores obtained for prostatic adenocarcinoma tissues compared with mean of composite scores obtained for adjacent benign prostatic tissue specimens.

compartment was substantially enhanced in PC tissue specimens as compared with normal and adjacent benign prostatic tissues (Figure 1A).

Table 1. Immunohistochemical analyses of MIC-1 expression in nonmalignant and malignant prostatic tissue specimens

Pathological diagnosis	Number of cases	Gleason score	Tumour stage	Positive staining for MIC-1	Mean of composite scores ^a	P-value ^b
Adjacent nonmalignant prostatic tissue	32	7–9	2–3			
Higher in adjacent benign vs normal prostatic tissues				59%	1.5 ± 0.3 vs 0.4 ± 0.3	P ≤ 0.005
Prostatic adenocarcinoma tissue	32	7–9	2–3			
Higher in PC vs normal prostatic tissues				84%	3.9 ± 0.4 vs 0.4 ± 0.3	P ≤ 0.0001
Higher in PC vs adjacent benign prostatic tissues				72%	3.9 ± 0.4 vs 1.5 ± 0.3	P ≤ 0.0001

Abbreviations: MIC-1 = macrophage inhibitory cytokine-1; PC = prostate cancer.
^aMean of composite scores ± s.e.
^bP-value indicates a significant difference between means of composite scores.

Investigation of the MIC-1 implication for the malignant behaviour and chemoresistant phenotype of PC3 cells. The results have indicated that the stimulation of parental PC3 cells expressing a low level of endogenous MIC-1 protein by 1 ng ml⁻¹ rhMIC-1, which is included in the range of the physiological serum concentrations of MIC-1 (≈ 0.7 ng ml⁻¹) (Brown *et al*, 2006), does not influence their proliferation but significantly increased ($P < 0.0001$) their invasive ability compared with untreated PC3 cells (Figures 2A and 3A). Interestingly, the treatment of starved PC3 cells with 1 ng ml⁻¹ rhMIC-1 was also accompanied by a decreased expression of E-cadherin, which was mainly localised in the cytoplasm, concomitant with enhanced expression levels of N-cadherin and vimentin, typical characteristics linked to the induction of the EMT process (Figures 3B and C). The stimulation of starved PC3 cells with rhMIC-1 was also associated with a more intense F-actin staining and cytoskeleton reorganisation, resulting in the formation of more cytoplasmic projections, including microspikes, filopodia- and lamellipodia-like protrusions as compared with untreated PC3 cells (Figure 3B). Moreover, the promoting effects induced by exogenous rhMIC-1 on the invasiveness and acquisition of a EMT phenotype by PC3 cells was significantly inhibited ($P < 0.0001$) by a selective and potent inhibitor of type I ALK including ALK4, ALK5 and ALK7 of the TGF- β superfamily designated as SB431542 (Figures 3A–C). We have also observed that rhMIC-1-stimulated PC3 cells were less sensitive to the antiproliferative and anti-invasive effects induced by docetaxel as compared with untreated PC3 cells (Figures 2A and 3A). The values of the half-maximal inhibitory concentration (IC₅₀) obtained for antiproliferative effect induced by docetaxel on rhMIC-1-stimulated PC3 (7.6 ± 0.6 nM) was significantly higher than the value for untreated PC3 (4.0 ± 0.3 nM; $P < 0.01$).

Estimation of antiproliferative and anti-invasive effects induced by docetaxel on PC cells expressing a low or a high level of the MIC-1 protein. The results from MTT tests and *in vitro* invasion assays have indicated that PC3-MIC-1 cells engineered for overexpressing MIC-1 were less sensitive to the antiproliferative and anti-invasive effects induced by docetaxel as compared with PC3-Vect cells expressing a low level of MIC-1 (Figures 2B, C and 3D). The IC₅₀ value obtained for antiproliferative effect induced by docetaxel on PC3-MIC-1 (6.7 ± 0.6 nM) was significantly higher than the value for PC3-Vect (3.4 ± 0.2 nM; $P < 0.0001$). In contrast, the MIC-1 downregulation in LNCaP-LN3-siMIC-1 and PC3M-LN4-siMIC-1 cells was accompanied by an enhanced sensitivity of PC cells to the growth inhibitory effects induced by docetaxel relative to LNCaP-LN3-Con and PC3M-LN4-Con cells expressing a high level of MIC-1, respectively (Figures 2B, D and E). Specifically, the IC₅₀ value obtained for the antiproliferative effect induced by docetaxel on LNCaP-LN3-siMIC-1 (5.2 ± 0.8 nM) or

PC3M-LN4-siMIC-1 cells (4.0 ± 0.6 nM) was significantly lower than the value for LNCaP-LN3-Con (8.5 ± 1.5 nM; $P < 0.0001$) or PC3M-LN4-Con cells (6.0 ± 0.8 nM; $P < 0.01$), respectively. In addition, the data from FACS analyses have also revealed that the 2-day docetaxel treatment of MIC-1-silenced PC3M-LN4-siMIC-1 cells resulted in a higher percentage of PC cells in the G2/M phase in conjunction with a reduction in the number of cells in the S phase relative to PC3M-LN4-Con cells (Figure 2F and Supplementary Table S1). Moreover, the data from *in vitro* invasion assays have indicated that LNCaP-LN3-siMIC-1 and PC3M-LN4-siMIC-1 cells displayed a weaker invasive ability and were more sensitive to the anti-invasive effect induced by docetaxel than LNCaP-LN3-Con and PC3M-LN4-Con cells (Figure 3E and F; $P < 0.0001$), respectively.

Determination of the apoptotic effect induced by docetaxel on PC cells expressing a low or high level of MIC-1 protein. The apoptotic effect induced by docetaxel on PC cells was estimated by FACS analyses and the apoptotic cell number in the sub-G1 phase was quantified. As shown in Figure 4, the increasing concentrations of docetaxel induced a higher rate of apoptotic death on PC3-Vect expressing a low level of MIC-1 than on PC3-MIC-1 cells overexpressing MIC-1. More specifically, 10 nM docetaxel caused a higher proportion of apoptotic death of PC3-Vect (63 ± 1%) as compared with PC3-MIC-1 (39 ± 3%; $P < 0.0001$; Figure 4B). Importantly, MIC-1-silenced LNCaP-LN3-siMIC-1 and PC3M-LN4-siMIC-1 cells were also more responsive to the apoptotic effect induced by docetaxel than LNCaP-LN3-Con and PC3M-LN4-Con cells expressing high level of endogenous MIC-1, respectively (Figure 4). More specifically, 10 nM docetaxel induced a higher rate of apoptosis in LNCaP-LN3-siMIC-1 (53 ± 5%) and PC3M-LN4-siMIC-1 cells (52 ± 3%) as compared with LNCaP-LN3-Con (38 ± 1%, $P < 0.0001$) and PC3M-LN4-Con cells (31 ± 1%, $P < 0.0001$), respectively (Figure 4B).

Establishment of the role of mitochondrial and caspase pathways in the apoptotic effect induced by docetaxel on PC3M-LN4 cells expressing a low or high level of MIC-1 protein. An estimation of the effects of docetaxel treatment on the MMP of PC3M-LN4-Con cells and PC3M-LN4-siMIC-1 cells was performed by FACS analyses. Moreover, the continuous treatment of the PC cells for 4 days with 2–10 nM docetaxel was accompanied by a decrease of MMP, as indicated by the shoulder of the peak and enhanced percentages of depolarised cells as compared with stained PC cells that were untreated (control) (Figures 5A and B). The docetaxel treatment of MIC-1-silenced PC3M-LN4-siMIC-1 cells was, however, accompanied by a higher mitochondrial membrane depolarising effect and percentage of depolarised cells as compared with PC3M-LN4-Con cells overexpressing MIC-1 (Figures 5A and B). More specifically, the data of the percentage of

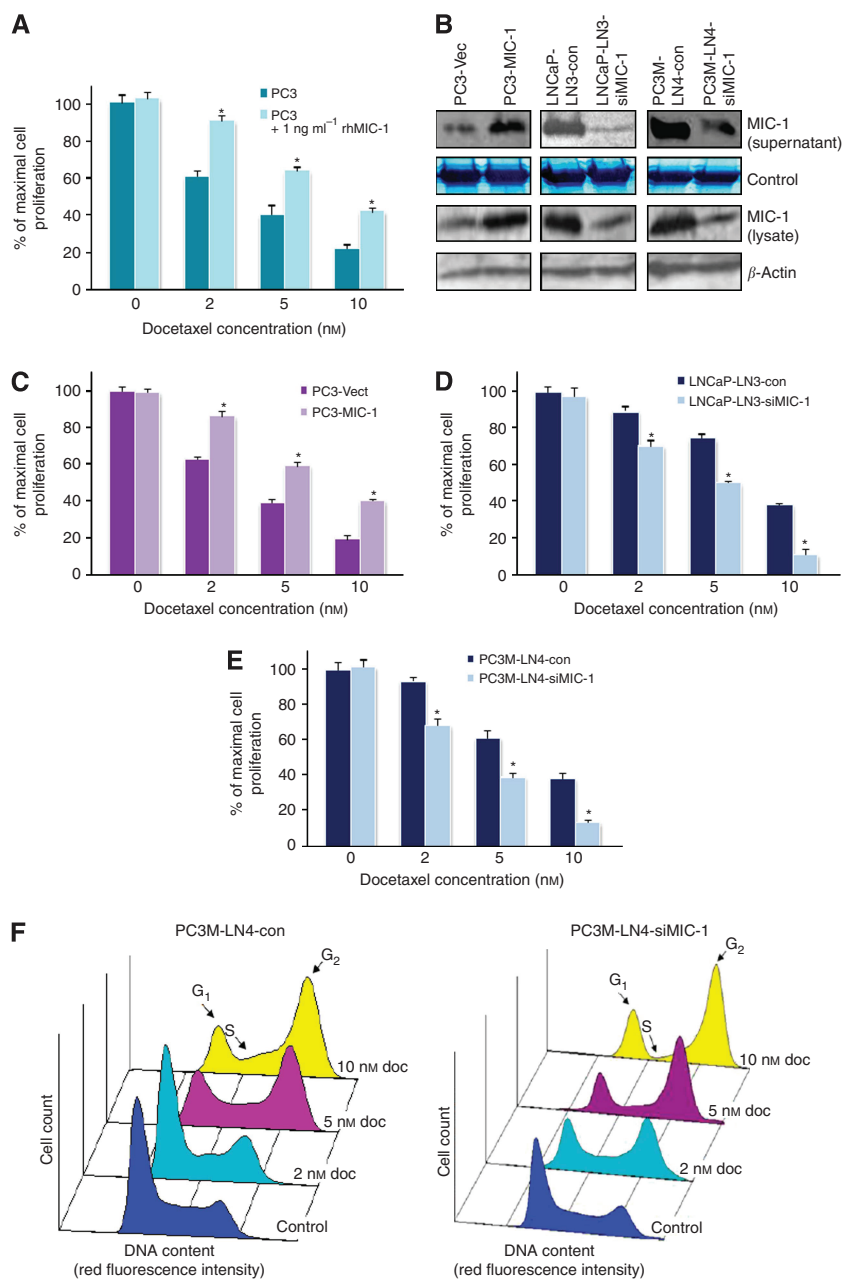


Figure 2. Effect of the MIC-1 protein on the antiproliferative effect induced by docetaxel on metastatic and AI PC cell lines. The PC cells were untreated (control) or treated with indicated docetaxel (Doc) concentrations for 2 days and the cell proliferation was evaluated by MTT assays and FACS analyses. **(A)** Data obtained by MTT assay for parental PC3 cells expressing a low level of MIC-1 untreated or treated with exogenous rhMIC-1 protein. **(B)** Immunoblot analyses of the expression levels of MIC-1 protein in culture supernatant and lysates from tested PC cell lines. Data obtained by MTT assays for **(C)** PC3-vect expressing low level of endogenous MIC-1 vs PC3-MIC-1 engineered for overexpressing MIC-1 and **(D)** LNCaP-LN3-Con and **(E)** PC3M-LN4-Con cells overexpressing MIC-1 vs MIC-1-silenced LNCaP-LN3-siMIC-1 and PC3M-LN4-siMIC-1 cells, respectively. **(F)** FACS analyses of number of PC cells in the cell cycle phase for PC3M-LN4-Con vs PC3M-LN4-siMIC-1 cells untreated or treated with indicated docetaxel concentrations for 2 days.

depolarised cells induced by 10 nM docetaxel on PC3M-LN4-siMIC-1 cells ($58 \pm 6\%$) were significantly more elevated as compared with the values obtained for PC3M-LN4-Con cells ($34 \pm 2\%$; $P < 0.0001$; Figure 5B).

Western blot analyses have also indicated that MIC-1-silenced PC3M-LN4-siMIC-1 cells treated with 10 nM docetaxel showed a greater amount of cytosolic cytochrome, cleaved fragments of caspase-9 and caspase-3 and PARP, and DNA laddering than PC3M-LN4-Con cells (Figures 5C and D). Moreover, the results from FACS analyses have revealed that the broad-spectrum caspase

inhibitor Z-VAD-FMK at $50 \mu\text{M}$ markedly abrogated the percentage of apoptotic death induced by docetaxel on all tested PC cells (Figure 4B).

Characterisation of SP and non-SP PC3M-LN4 cells and the estimation of cytotoxic effects induced by the downregulation of MIC-1 and docetaxel treatment. The results from FACS analyses have indicated the presence of a small SP cell subpopulation representing $\sim 0.87\%$ of the total mass of PC3M-LN4 cells (Figure 6A). The SP cell fraction was significantly reduced in the

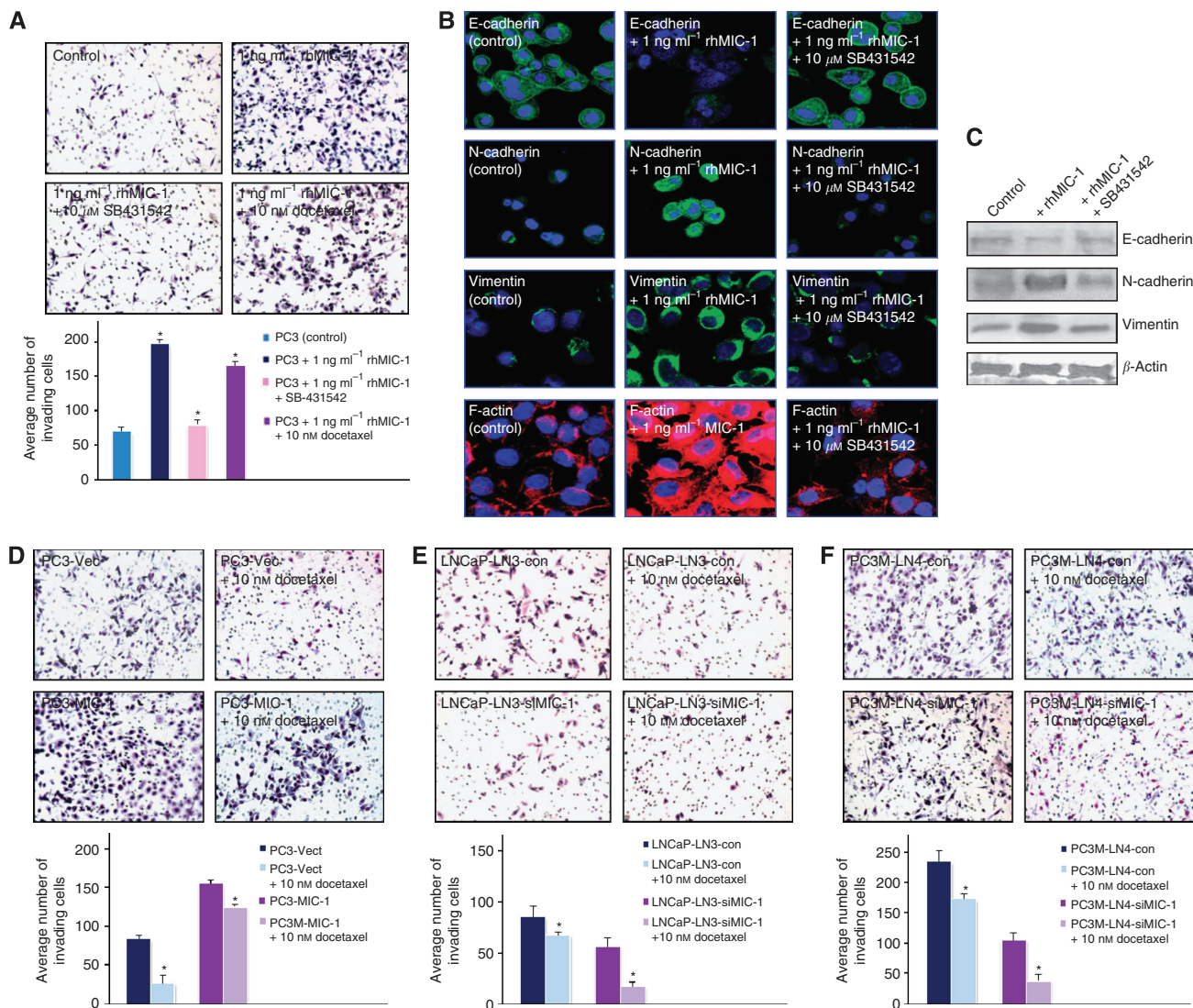


Figure 3. Effect of the MIC-1 protein on the invasive ability of PC cells and the anti-invasive effect induced by docetaxel treatment on PC cell lines expressing low and high levels of the MIC-1 protein. The PC cells were untreated (control) or treated with the indicated agents, plated on matrigel-coated membrane for invasion assays and incubated for 24 h. Data of the invasive ability obtained for (A) parental PC3 cells after a treatment with 1 ng ml⁻¹ rhMIC-1 in the absence or presence of 10 μM SB431542 or 10 nM docetaxel. The results from comparative analyses by (B) confocal microscopy and (C) western blot of the effect induced by a treatment of starved PC3 cells with 1 ng ml⁻¹ rhMIC-1 in the absence or presence of 10 μM SB431542 on expression levels and intracellular localisation of different gene products associated with the EMT process. Data of the invasive ability obtained for (D) PC3-Vect cells expressing a low level of MIC-1 vs PC3-MIC-1 cells engineered for overexpressing MIC-1 protein, and (E) scrambled LNCaP-LN3-Con and (F) PC3M-LN4-Con cells overexpressing high levels of endogenous MIC-1 vs MIC-1-silenced LNCaP-LN3-siMIC-1 and PC3M-LN4-siMIC-1 cells, respectively.

presence of the ABC transporter inhibitor, 50 μM verapamil, indicating that the SP phenotype may be associated with a high expression of ABC multidrug efflux pumps (Figure 6A). Moreover, the FACS analyses after staining of PC3M-LN4 cells with phycoerythrin-labelled CD133 antibody have also indicated the presence of a small PC3M-LN4 cell population expressing a high level of a CD133 stem cell-like marker corresponding to ~0.79% of the total PC3M-LN4 cell mass (Figure 6B). We have also observed that SP PC3M-LN4 cells displayed a greater clone formation efficacy and were able to generate many dense prostaspheres with a large size (72 ± 3 prostaspheres for 500 plated SP cells) in serum free-medium under ultra-low attachment plate as compared with non-SP cells (Figures 6C and D). Moreover, SP PC3M-LN4 cells also expressed higher levels of stem cell-like markers, including CD133, CD44 and ABCG2

multidrug transporter, and EMT-associated molecules, such as N-cadherin and vimentin, relative to the non-SP cell fraction (Figures 6E–G). Interestingly, SP and non-SP PC3M-LN4 cell fractions also expressed significant levels of MIC-1, EGFR and its phosphorylated Tyr¹¹⁷³-pEGFR form and F-actin (Figures 6E and G).

Importantly, the results from FACS analyses have also revealed that the treatment of PC3M-LN4-Con cells with 10 nM docetaxel for 4 days was accompanied by a significant increase in the percentage of viable SP cells, whereas the number of cells in the bulk PC cell mass was reduced as compared with the nontreated cells (Figure 6H). The MIC-1 silencing in PC3M-LN4-siMIC-1 cells was, however, accompanied by a significant decrease of viable SP and the bulk PC cell mass, including non-SP cells (Figure 6H). Of therapeutic interest, the docetaxel treatment of

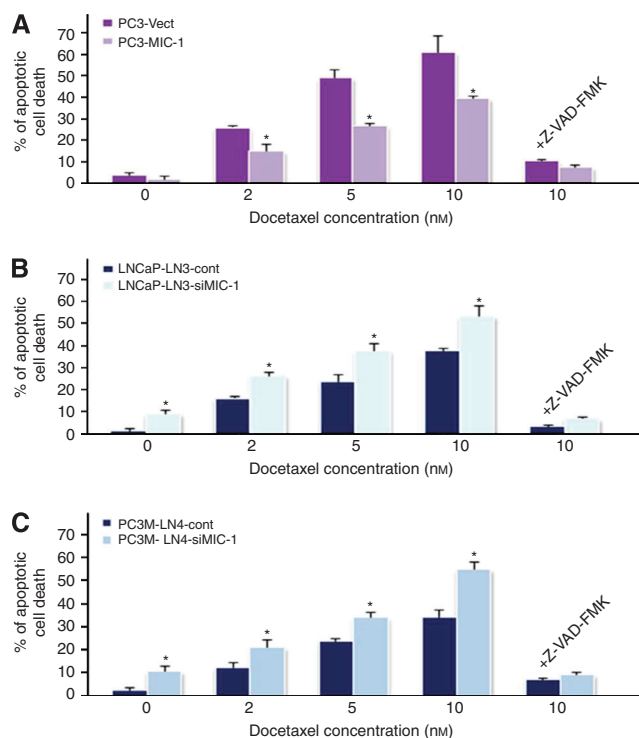


Figure 4. Fluorescence-activated cell sorting (FACS) analyses of the apoptotic effect induced by docetaxel on PC cell lines expressing low and high levels of the MIC-1 protein. Plots showing the percentages of apoptotic cell death induced after 4 days of treatment of PC cells with indicated docetaxel concentrations in the absence or presence of broad caspase inhibitor, Z-VAD-FMK, at 50 μ M, which was estimated by the number of apoptotic cells detected in the sub-G1 phase by FACS analyses. Quantitative data obtained for **(A)** PC3-Vect cells expressing a low level of MIC-1 vs PC3-MIC-1 cells engineered for overexpressing MIC-1 protein, and **(B and C)** scrambled LNCaP-LN3-Con and PC3M-LN4-Con cells overexpressing high levels of endogenous MIC-1 vs MIC-1-silenced LNCaP-LN3-siMIC-1 and PC3M-LN4-siMIC-1 cells, respectively.

PC3M-LN4-siMIC-1 cells was also associated with a greater decrease in the percentage of viable SP cells as well as the number of cells in the bulk PC cell mass, including non-SP cells, relative to PC3M-LN4-Con cells treated with 10 nM docetaxel (Figure 6H).

DISCUSSION

The results of the present investigation have provided new lines of experimental evidence for a direct association of the enhanced expression of secreted MIC-1 protein with the acquisition of aggressive and chemoresistant phenotypes by PC cells during disease progression. More specifically, the data from immunohistochemical analyses have revealed that the expression of the MIC-1 protein was enhanced in PC cells in 83% and 72% of primary prostatic adenocarcinomas from PC patients (Gleason scores = 7–9) as compared with normal prostatic tissues of biopsy and adjacent benign prostatic tissues from the same patients, respectively (Figures 1A and B and Table 1). In addition, the data from western blot have also indicated that the highly metastatic and AI LNCaP-LN3 cells expressing a functional androgen receptor (AR) and AR⁻ PC3M-LN4 cell line, which has previously been observed to display a higher propensity to metastasise to bones than the PC3 cell line, expressed a high level of MIC-1 (Figure 2B) (Pettaway

et al, 1996). Together, these data support numerous prior studies indicating that a progressive increase of the MIC-1 level occurs in PC cells during prostate carcinogenesis and PC progression of androgen-sensitive to androgen-independent and metastatic disease states (Karan *et al*, 2002, 2003; Nakamura *et al*, 2003; Welsh *et al*, 2003; Cheung *et al*, 2004; Bauskin *et al*, 2005; Brown *et al*, 2006; Chen *et al*, 2007; Huang *et al*, 2007; Patrikainen *et al*, 2007; Selander *et al*, 2007; Brown *et al*, 2009; Wakchoure *et al*, 2009; Zhao *et al*, 2009; Senapati *et al*, 2010; Mimeault *et al*, 2012). More specifically, a significant increase of MIC-1/GDF15 expression, at both the mRNA and mature protein level, has been detected in prostatic hyperplasia and prostatic intraepithelial neoplastic (PIN) lesions formed in the LBT Tag 12T-7s transgenic mouse model, a modified SV40 early region driven by the prostate-specific rat probasin promoter, and associated with a stimulation of prostatic epithelial cell proliferation (Kasper *et al*, 1998; Noorali *et al*, 2007). These data suggest that an enhanced expression of the mature MIC-1/GDF-15 form may constitute an early transforming event during prostate carcinogenesis. Moreover, the enhanced expression of MIC-1 in prostatic adenocarcinoma tissues and/or serum samples has been positively correlated with the presence of metastatic PCs and poor prognosis of PC patients as a result of treatment resistance (Karan *et al*, 2002; Nakamura *et al*, 2003; Welsh *et al*, 2003; Cheung *et al*, 2004; Bauskin *et al*, 2005; Brown *et al*, 2006; Huang *et al*, 2007; Patrikainen *et al*, 2007; Selander *et al*, 2007; Brown *et al*, 2009; Zhao *et al*, 2009; Mimeault *et al*, 2010a). In addition, the results of our recent work have also revealed that the expression levels of MIC-1 protein were increased in CD133⁺ PC cell subpopulation and the bulk mass of CD133⁻ PC cells in prostatic adenocarcinoma tissues as well as in PC cells detected in bone metastasis tissue specimens from PC patients relative to normal prostate tissues (Mimeault *et al*, 2012). Altogether, these observations suggest that an enhanced expression of MIC-1 frequently occurs in PC cells during PC progression and in bone metastases and may contribute to disease relapse. This supports great interest to further investigate the possibility to use MIC-1 as prognostic indicator, alone or in combination with other current clinical biomarkers, to predict the risk of PC progression to AI, metastatic and recurrent disease states.

In addition, the results have also revealed that an increase of the expression level of secreted MIC-1 cytokine may be associated with the acquisition of a more malignant behaviour by metastatic and AI PC cells. Particularly, we have observed that the exogenous rhMIC-1 treatment or ectopic overexpression of MIC-1 in PC3 cells was accompanied by a significant increase of their invasive ability, whereas the MIC-1 downregulation in highly metastatic LNCaP-LN3 and PC3M-LN4 cells markedly decreased their invasiveness (Figures 3A, D, E and F). Our results have also indicated that the treatment of PC3 cells with rhMIC-1 upregulated the expression of the EMT programme-associated molecules, including mesenchymal markers, N-cadherin and vimentin, concomitant with a decreased expression of epithelial marker E-cadherin. Moreover, the treatment of PC3 cells with rhMIC-1 also induced a F-actin reorganisation, at least in part, via the activation of type I ALK receptors of TGF- β superfamily (Figures 3B and C). These data support previous studies indicating that the secreted MIC-1 protein may mediate its effects through TGF- β superfamily receptors, and TGF- β family members can cooperate with other growth factors including EGF to induce a partial or full EMT programme in cancer cells, including PC3 cells (Tan *et al*, 2000; Xu *et al*, 2006; Johnen *et al*, 2007; Soto-Cerrato *et al*, 2007; Kong *et al*, 2008; Otero-Marah *et al*, 2008; Ago *et al*, 2010; Lenferink *et al*, 2010; Mimeault *et al*, 2010a, b; Lim *et al*, 2011). These observations are also in agreement with prior investigations that have shown that the MIC-1 overexpression in metastatic and androgen-sensitive AR⁺ LNCaP-C33 and AI AR⁺ LNCaP-LN3 and AR⁻ PC3 cells enhanced their migratory and invasive abilities

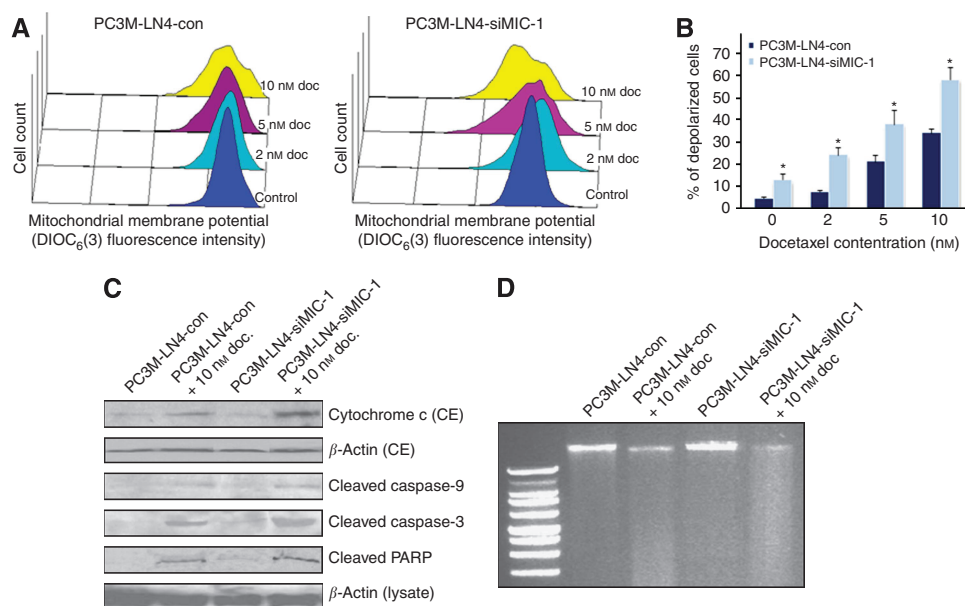


Figure 5. Stimulatory effect induced by docetaxel on mitochondrial membrane depolarisation, cytosolic cytochrome c releasing, caspase pathway activation and DNA fragmentation in PC3M-LN4-Con and MIC-1-silenced PC3M-LN4-siMIC-1 cells. (A) Representative profiles of effect induced by docetaxel on MMP in PC cells are shown. (B) Plots showing the percentage of depolarised PC cells induced after treatment with different docetaxel concentrations. (C) Western blot analyses of the amounts of cytochrome c released into cytosol, cleaved fragments of caspase-9 and caspase-3 and PARP, and (D) DNA fragmentation detected by agarose gel electrophoresis in PC cells untreated (control) or treated with 10 nM docetaxel for 4 days.

in vitro (Chen *et al*, 2007; Senapati *et al*, 2010). Importantly, it has also been reported that the intraprostatic orthotopically implanted PC3 cells engineered for overexpressing MIC-1 in nude mice developed metastases in regional and distant organs, whereas no metastasis was seen in the animal group implanted with empty-vector-transfected PC3 cells (Senapati *et al*, 2010). Hence, these results suggest that MIC-1 can provide critical functions for invasion and metastatic spread to distant tissues including lymph nodes and bones of PC cells, at least in part, by inducing the EMT programme via TGF- β superfamily receptors.

Although the development of early detection tests had led to an improvement in prognosis for patients with localised PCs treated with prostatectomy, AI lesions may eventually develop and progress despite low levels of circulating androgens (Tannock *et al*, 2004; Mimeault and Batra, 2006; Freedland, 2010). Patients with locally advanced or metastatic CRPCs, resistant to anti-hormonal therapy, radiotherapy and first-line systemic docetaxel-based chemotherapies, are usually dead after 12 to 19 months (Petrylak *et al*, 2004; Tannock *et al*, 2004; Mimeault and Batra, 2006; Freedland, 2010; Siegel *et al*, 2012). In this regard, we have shown that a downregulation of the MIC-1 expression in highly metastatic LNCaP-LN3-siMIC-1 and PC3M-LN4-siMIC-1 cells was accompanied by an increase of their sensitivity to antiproliferative and anti-invasive effects induced by the current chemotherapeutic drug, docetaxel (Figures 2 and 3 and Supplementary Table S1). The MIC-1-silenced LNCaP-LN3-siMIC-1 and PC3M-LN4-siMIC-1 cells were also more sensitive to the apoptotic effect induced by docetaxel through a mitochondrial- and caspase activation-dependent pathway (Figures 4 and 5). These data support prior studies that have indicated that MIC-1 can contribute to aggressive behaviour and docetaxel resistance of PC cells (Huang *et al*, 2007; Zhao *et al*, 2009). For instance, it has been reported that PC3-Rx cells made resistant to docetaxel exhibited a greater expression level of MIC-1 relative to the parental PC3 cell line (Zhao *et al*, 2009). Also, the overexpression of MIC-1 in metastatic and AI PC3 and DU145 cells or a treatment

with exogenous rhMIC-1 enhanced their resistance to cytotoxic effects induced by docetaxel or mitoxantrone *in vitro* (Huang *et al*, 2007; Zhao *et al*, 2009). Moreover, it has also been observed that the MIC-1 concentrations detected in serum/plasma were more elevated after docetaxel treatment and associated with the PC progression and a shorter survival of PC patients (Huang *et al*, 2007; Zhao *et al*, 2009). In addition, higher serum levels of MIC-1 were also detected in PC patients with bone metastases as compared with patients without bone metastases (Selander *et al*, 2007). The patients who developed bone relapse had significantly higher serum levels of MIC-1 relative to patients who did not (Selander *et al*, 2007). It has also been noticed that PC cells expressing MIC-1 can induce mixed osteoblastic/osteolytic lesions, suggesting a critical role for secreted MIC-1 in the development of these pathological complications of bone metastases (Wakchoure *et al*, 2009).

Importantly, numerous recent studies have revealed that distinct subsets of highly tumourigenic PC stem/progenitor cells expressing stem cell-like markers such as CD133, CD44^{high}, ALDH^{high}, Oct-3/4, Nanog, Sox-2 and/or ABCG2 and EMT-associated molecules but undetectable or low level of AR and prostate-specific antigen (PSA) can be more resistant than the bulk mass of PC cells to current androgen deprivation and chemotherapy (Patrawala *et al*, 2007; Birnie *et al*, 2008; Duhagon *et al*, 2010; Kong *et al*, 2010; Liu *et al*, 2010; Mimeault and Batra, 2010b; Jeter *et al*, 2011; Mimeault and Batra, 2011a; Rajasekhar *et al*, 2011; Dubrovskaya *et al*, 2012; Germann *et al*, 2012; Lee *et al*, 2013; Mimeault *et al*, 2012; Sun *et al*, 2012). Consequently, the persistence and enrichment of PC stem/progenitor cells after treatment initiation may lead to the tumour re-growth, metastases and disease relapse (Patrawala *et al*, 2007; Klarmann *et al*, 2009; Liu *et al*, 2010; Mimeault *et al*, 2010a; Jeter *et al*, 2011; Mimeault and Batra, 2011a; Dubrovskaya *et al*, 2012; Germann *et al*, 2012; Lee *et al*, 2013; Mimeault *et al*, 2012; Sun *et al*, 2012). Of therapeutic interest, the results of the present study have revealed that the downregulation of MIC-1 was effective in enhancing the sensitivity of the SP PC3M-LN4 cell subpopulation

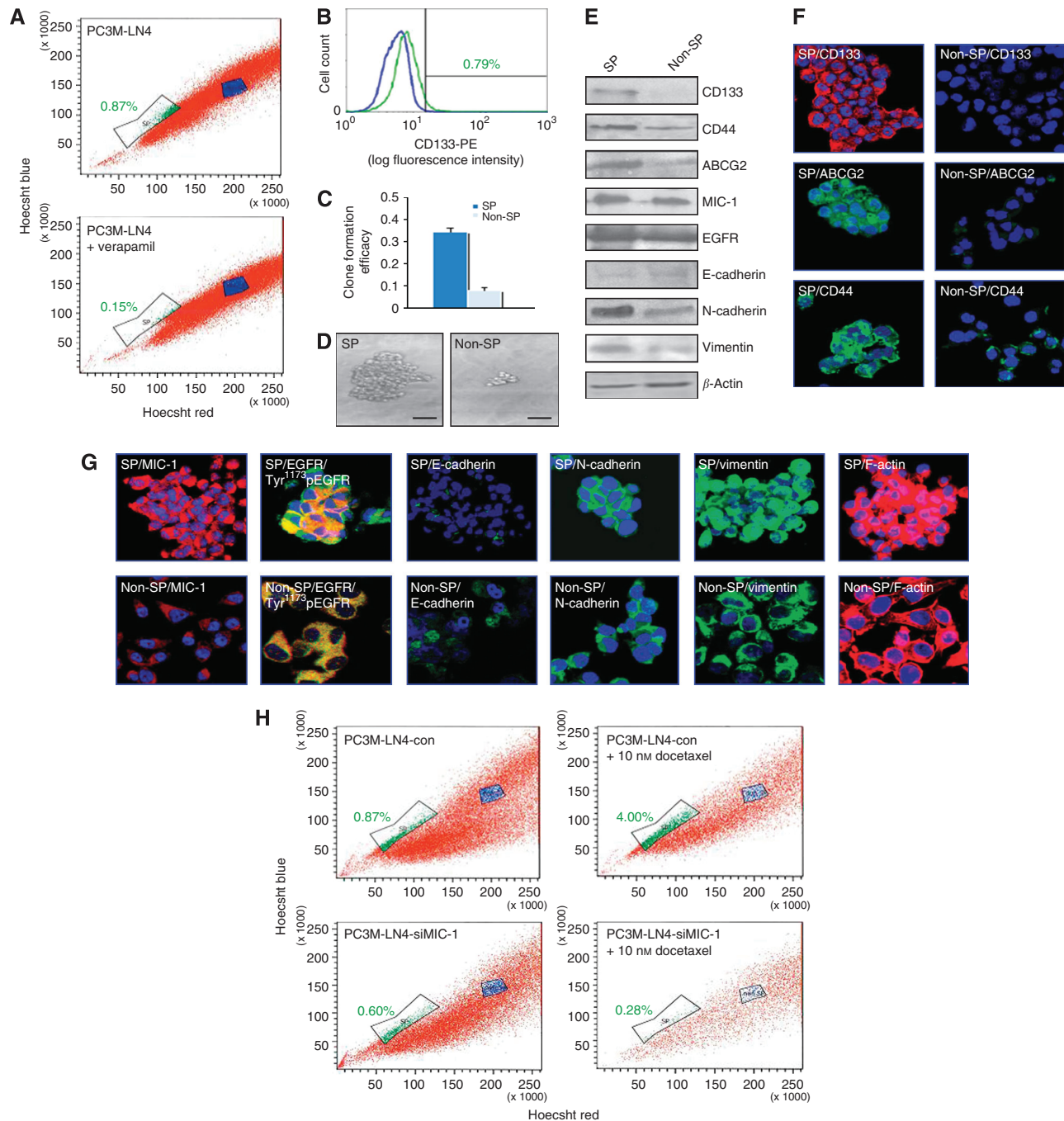


Figure 6. Characterisation of phenotypic and functional features of SP and non-SP PC3M-LN4 cell fractions and the implication of MIC-1 in their sensitivity to the cytotoxic effect induced by docetaxel. **(A)** Hoechst dye efflux profiles obtained for parental PC3M-LN4 cells stained with fluorescent Hoechst dye in the absence or presence of 50 μ M verapamil showing SP cells (green) and the non-SP fraction (blue) and **(B)** FACS profiles obtained after staining of PC3M-LN4 cells with phycoerythrin-labelled anti-CD133 antibody. **(C)** Clone formation efficacy of SP and non-SP PC3M-LN4 fractions and **(D)** representative pictures of dense prostatespheres formed by SP PC3M-LN4 cells as compared with small aggregates formed by non-SP PC3M-LN4 cells. **(E–G)** Comparative western blot and immunofluorescence analyses of expression levels of different markers in SP and non-SP PC3M-LN4 cell fractions. **(H)** Hoechst dye efflux profiles obtained for PC3M-LN4-Con cells overexpressing endogenous MIC-1 and MIC-1-silenced PC3M-LN4-siMIC-1 cells untreated or treated with 10 nM docetaxel for 4 days.

endowed with a high self-renewal and expressing high levels of stem cell-like markers and EMT-associated molecules as well as the bulk mass of PC cells including non-SP cells to cytotoxic effects of docetaxel (Figure 6). Hence, these observations support great interest to target the MIC-1 signalling cascade to eradicate AI, metastatic and chemoresistant PC stem/progenitor cells endowed with stem cell-like and EMT properties to counteract disease

progression to metastatic CRPCs. In this regard, the data of prior microarray analyses have also indicated that the prostatespheres formed by LNCaP cells in serum-free medium expressed a higher level of MIC-1/GDF-15 as compared with LNCaP cells grown in medium containing 10% serum (Duhagon *et al*, 2010). It has also been reported that the inhibition of LuCaP35 tumour growth induced by androgen-deprivation therapy was associated with

enhanced expression levels of stem cell-like markers and EMT-associated molecules such as N-cadherin, vimentin and twist and activated TGF- β signalling pathway in tumours (Sun *et al*, 2012). Moreover, LNCaP cells cultured in medium containing charcoal-stripped serum (CSS) also exhibited a higher resistance to docetaxel than LNCaP cells grown in CSS plus α -dihydrotestosterone (Sun *et al*, 2012). Interestingly, the data from a recent study have also indicated that PSA^{-low}/AR^{-low} PC or PSA^{-low}/AR⁺ cells, which harbour a subpopulation of highly tumorigenic CD44⁺/ α ₂ β ₁⁺/ALDH⁺ PC cell, detected in LNCaP, LaPC9 or primary PC cells displayed a higher self-renewal and tumorigenic abilities than PSA⁺ PC cells (Qin *et al*, 2012). In addition, PSA^{-low} PC cells were also more resistant to androgen-deprivation therapy and chemotherapy, including paclitaxel, than the bulk mass of differentiated PSA⁺ PC cells *in vitro* and *in vivo* (Qin *et al*, 2012).

Taken together, the results of the present investigation have revealed that the overexpression of MIC-1 in metastatic and androgen-sensitive and AI AR⁺ and AR⁻ PC cells can contribute to their acquisition of a more aggressive behaviour, EMT phenotypes and docetaxel resistance. Importantly, the data have also indicated that the downregulation of MIC-1 in AI PC cells, including PC stem/progenitor cells, may represent a promising therapeutic strategy to improve the anticarcinogenic efficacy of docetaxel, by eradicating the total PC cell mass and thereby preventing disease progression and relapse, and the death of PC patients.

ACKNOWLEDGEMENTS

The authors on this work are supported, in part, by the grant from National Institutes of Health (R01CA138791) and Department of Defense (PC074289) for prostate cancer research. We thank the Molecular Biology Core Facility at the University of Nebraska Medical Center for confocal and FACS analyses. The technical support from Erik Moore and Kavita Mallya is greatly appreciated.

REFERENCES

- Ago T, Kuroda J, Pain J, Fu C, Li H, Sadoshima J (2010) Upregulation of Nox4 by hypertrophic stimuli promotes apoptosis and mitochondrial dysfunction in cardiac myocytes. *Circ Res* **106**: 1253–1264.
- Bauskin AR, Brown DA, Junankar S, Rasiah KK, Eggleston S, Hunter M, Liu T, Smith D, Kuffner T, Pankhurst GJ, Johnen H, Russell PJ, Barret W, Stricker PD, Grygiel JJ, Kench JG, Henshall SM, Sutherland RL, Breit SN (2005) The propeptide mediates formation of stromal stores of PROMIC-1: role in determining prostate cancer outcome. *Cancer Res* **65**: 2330–2336.
- Birnie R, Bryce SD, Roome C, Dussupt V, Droop A, Lang SH, Berry PA, Hyde CF, Lewis JL, Stower MJ, Maitland NJ, Collins AT (2008) Gene expression profiling of human prostate cancer stem cells reveals a pro-inflammatory phenotype and the importance of extracellular matrix interactions. *Genome Biol* **9**: R83.
- Boyle GM, Pedley J, Martyn AC, Banducci KJ, Stratton GM, Brown DA, Breit SN, Parsons PG (2009) Macrophage inhibitory cytokine-1 is overexpressed in malignant melanoma and is associated with tumorigenicity. *J Invest Dermatol* **129**: 383–391.
- Brown DA, Lindmark F, Stattin P, Balter K, Adami HO, Zheng SL, Xu J, Isaacs WB, Gronberg H, Breit SN, Wiklund FE (2009) Macrophage inhibitory cytokine 1: a new prognostic marker in prostate cancer. *Clin Cancer Res* **15**: 6658–6664.
- Brown DA, Stephan C, Ward RL, Law M, Hunter M, Bauskin AR, Amin J, Jung K, Diamandis EP, Hampton GM, Russell PJ, Giles GG, Breit SN (2006) Measurement of serum levels of macrophage inhibitory cytokine 1 combined with prostate-specific antigen improves prostate cancer diagnosis. *Clin Cancer Res* **12**: 89–96.
- Chen SJ, Karan D, Johansson SL, Lin FF, Zeckser J, Singh AP, Batra SK, Lin MF (2007) Prostate-derived factor as a paracrine and autocrine factor for the proliferation of androgen receptor-positive human prostate cancer cells. *Prostate* **67**: 557–571.
- Cheung PK, Woolcock B, Adomat H, Sutcliffe M, Bainbridge TC, Jones EC, Webber D, Kinahan T, Sadar M, Gleave ME, Vielkind J (2004) Protein profiling of microdissected prostate tissue links growth differentiation factor 15 to prostate carcinogenesis. *Cancer Res* **64**: 5929–5933.
- Dubrovskaya A, Elliott J, Salamone RJ, Telegeev GD, Stakhovskiy AE, Schepotin IB, Yan F, Wang Y, Bouchez LC, Kularatne SA, Watson J, Trussell C, Reddy VA, Cho CY, Schultz PG (2012) CXCR4 expression in prostate cancer progenitor cells. *PLoS ONE* **7**: e31226.
- Duhagon MA, Hurt EM, Sotelo-Silveira JR, Zhang X, Farrar WL (2010) Genomic profiling of tumor initiating prostatespheres. *BMC Genomics* **11**: 324.
- Freedland SJ (2010) Screening, risk assessment, and the approach to therapy in patients with prostate cancer. *Cancer* **117**: 1123–1135.
- Germann M, Wetterwald A, Guzman-Ramirez N, van der Pluijm G, Culig Z, Cecchini MG, Williams ED, Thalmann GN (2012) Stem-like cells with luminal progenitor phenotype survive castration in human prostate cancer. *Stem Cells* **30**: 1076–1086.
- Huang CY, Beer TM, Higano CS, True LD, Vessella R, Lange PH, Garzotto M, Nelson PS (2007) Molecular alterations in prostate carcinomas that associate with *in vivo* exposure to chemotherapy: identification of a cytoprotective mechanism involving growth differentiation factor 15. *Clin Cancer Res* **13**: 5825–5833.
- Huh SJ, Chung CY, Sharma A, Robertson GP (2010) Macrophage inhibitory cytokine-1 regulates melanoma vascular development. *Am J Pathol* **176**: 2948–2957.
- Jeter CR, Liu B, Liu X, Chen X, Liu C, Calhoun-Davis T, Repass J, Zaehres H, Shen JJ, Tang DG (2011) NANOG promotes cancer stem cell characteristics and prostate cancer resistance to androgen deprivation. *Oncogene* **30**: 3833–3845.
- Johnen H, Lin S, Kuffner T, Brown DA, Tsai VW, Bauskin AR, Wu L, Pankhurst G, Jiang L, Junankar S, Hunter M, Fairlie WD, Lee NJ, Enriquez RF, Baldock PA, Corey E, Apple FS, Murakami MM, Lin EJ, Wang C, During MJ, Sainsbury A, Herzog H, Breit SN (2007) Tumor-induced anorexia and weight loss are mediated by the TGF-beta superfamily cytokine MIC-1. *Nat Med* **13**: 1333–1340.
- Karan D, Chen SJ, Johansson SL, Singh AP, Paralkar VM, Lin MF, Batra SK (2003) Dysregulated expression of MIC-1/PDF in human prostate tumor cells. *Biochem Biophys Res Commun* **305**: 598–604.
- Karan D, Kelly DL, Rizzino A, Lin MF, Batra SK (2002) Expression profile of differentially-regulated genes during progression of androgen-independent growth in human prostate cancer cells. *Carcinogenesis* **23**: 967–975.
- Kasper S, Sheppard PC, Yan Y, Pettigrew N, Borowsky AD, Prins GS, Dodd JG, Duckworth ML, Matusik RJ (1998) Development, progression, and androgen-dependence of prostate tumors in probasin-large T antigen transgenic mice: a model for prostate cancer. *Lab Invest* **78**: i–xv.
- Kim KK, Lee JJ, Yang Y, You KH, Lee JH (2008) Macrophage inhibitory cytokine-1 activates AKT and ERK-1/2 via the transactivation of ErbB2 in human breast and gastric cancer cells. *Carcinogenesis* **29**: 704–712.
- Klarmann GJ, Hurt EM, Mathews LA, Zhang X, Duhagon MA, Mistree T, Thomas SB, Farrar WL (2009) Invasive prostate cancer cells are tumor initiating cells that have a stem cell-like genomic signature. *Clin Exp Metastasis* **26**: 433–446.
- Kong D, Banerjee S, Ahmad A, Li Y, Wang Z, Sethi S, Sarkar FH (2010) Epithelial to mesenchymal transition is mechanistically linked with stem cell signatures in prostate cancer cells. *PLoS ONE* **5**: e12445.
- Kong D, Wang Z, Sarkar SH, Li Y, Banerjee S, Saliganan A, Kim HR, Cher ML, Sarkar FH (2008) Platelet-derived growth factor-D overexpression contributes to epithelial-mesenchymal transition of PC3 prostate cancer cells. *Stem Cells* **26**: 1425–1435.
- Lee DH, Yang Y, Lee SJ, Kim KY, Koo TH, Shin SM, Song KS, Lee YH, Kim YJ, Lee JJ, Choi I, Lee JH (2003) Macrophage inhibitory cytokine-1 induces the invasiveness of gastric cancer cells by up-regulating the urokinase-type plasminogen activator system. *Cancer Res* **63**: 4648–4655.
- Lee SO, Ma Z, Yeh CR, Luo J, Lin TH, Lai KP, Yamashita S, Liang L, Tian J, Li L, Jiang Q, Huang CK, Niu Y, Yeh S, Chang C (2013) New

- therapy targeting differential androgen receptor signaling in prostate cancer stem/progenitor vs non-stem/progenitor cells. *J Mol Cell Biol* 5: 4–26.
- Lenferink AE, Cantin C, Nantel A, Wang E, Durocher Y, Banville M, Paul-Roc B, Marcil A, Wilson MR, O'Connor-McCourt MD (2010) Transcriptome profiling of a TGF-beta-induced epithelial-to-mesenchymal transition reveals extracellular clusterin as a target for therapeutic antibodies. *Oncogene* 29: 831–844.
- Lim M, Chuong CM, Roy-Burman P (2011) PI3K, Erk signaling in BMP7-induced epithelial-mesenchymal transition (EMT) of PC-3 prostate cancer cells in 2- and 3-dimensional cultures. *Horm Cancer* 2: 298–309.
- Liu T, Bauskin AR, Zaunders J, Brown DA, Pankhurst S, Russell PJ, Breit SN (2003) Macrophage inhibitory cytokine 1 reduces cell adhesion and induces apoptosis in prostate cancer cells. *Cancer Res* 63: 5034–5040.
- Liu T, Xu F, Du X, Lai D, Liu T, Zhao Y, Huang Q, Jiang L, Huang W, Cheng W, Liu Z (2010) Establishment and characterization of multi-drug resistant, prostate carcinoma-initiating stem-like cells from human prostate cancer cell lines 22RV1. *Mol Cell Biochem* 340: 265–273.
- Mimeault M, Batra S (2009) Characterization of non-malignant and malignant prostatic stem/progenitor cells by Hoechst side population method. *Methods Mol Biol* 568: 139–149.
- Mimeault M, Batra SK (2006) Recent advances on multiple tumorigenic cascades involved in prostatic cancer progression and targeting therapies. *Carcinogenesis* 27: 1–22.
- Mimeault M, Batra SK (2010a) Divergent molecular mechanisms underlying the pleiotropic functions of macrophage inhibitory cytokine-1 in cancer. *J Cell Physiol* 224: 626–635.
- Mimeault M, Batra SK (2010b) Frequent deregulations in the hedgehog signaling network and cross-talks with the epidermal growth factor receptor pathway involved in cancer progression and targeted therapies. *Pharmacol Rev* 62: 497–524.
- Mimeault M, Batra SK (2011a) Animal models of prostate carcinogenesis underlining the critical implication of prostatic stem progenitor cells. *Biochim Biophys Acta* 1816: 25–37.
- Mimeault M, Batra SK (2011b) Frequent gene products and molecular pathways altered in prostate cancer- and metastasis-initiating cells and their progenies and novel promising multitargeted therapies. *Mol Med* 17: 949–964.
- Mimeault M, Johansson SL, Batra SK (2012) Pathobiological implications of the expression of EGFR, pAkt, NF-kB and MIC-1 in prostate cancer stem cells and their progenies. *PLoS ONE* 7: e31919.
- Mimeault M, Johansson SL, Henichart JP, Depreux P, Batra SK (2010a) Cytotoxic effects induced by docetaxel, gefitinib, and cyclopamine on side population and non-side population cell fractions from human invasive prostate cancer cells. *Mol Cancer Ther* 9: 617–630.
- Mimeault M, Johansson SL, Senapati S, Momi N, Chakraborty S, Batra SK (2010b) MUC4 down-regulation reverses chemoresistance of pancreatic cancer stem/progenitor cells and their progenies. *Cancer Lett* 295: 69–84.
- Mimeault M, Johansson SL, Venkatraman G, Moore E, Henichart JP, Depreux P, Lin MF, Batra SK (2007a) Combined targeting of epidermal growth factor receptor and hedgehog signaling by gefitinib and cyclopamine cooperatively improves the cytotoxic effects of docetaxel on metastatic prostate cancer cells. *Mol Cancer Ther* 6: 967–978.
- Mimeault M, Jouy N, Depreux P, Henichart JP (2005) Synergistic antiproliferative and apoptotic effects induced by mixed epidermal growth factor receptor inhibitor ZD1839 and nitric oxide donor in human prostatic cancer cell lines. *Prostate* 62: 187–199.
- Mimeault M, Moore E, Moniaux N, Henichart JP, Depreux P, Lin MF, Batra SK (2006) Cytotoxic effects induced by a combination of cyclopamine and gefitinib, the selective hedgehog and epidermal growth factor receptor signaling inhibitors, in prostate cancer cells. *Int J Cancer* 118: 1022–1031.
- Mimeault M, Venkatraman G, Johansson SL, Moore E, Henichart JP, Depreux P, Lin MF, Batra SK (2007b) Novel combination therapy against metastatic and androgen-independent prostate cancer by using gefitinib, tamoxifen and etoposide. *Int J Cancer* 120: 160–169.
- Nakamura T, Scorilas A, Stephan C, Yousef GM, Kristiansen G, Jung K, Diamandis EP (2003) Quantitative analysis of macrophage inhibitory cytokine-1 (MIC-1) gene expression in human prostatic tissues. *Br J Cancer* 88: 1101–1104.
- Noorali S, Kurita T, Woolcock B, de Algora TR, Lo M, Paralkar V, Hoodless P, Vieland J (2007) Dynamics of expression of growth differentiation factor 15 in normal and PIN development in the mouse. *Differentiation* 75: 325–336.
- Odero-Marah VA, Wang R, Chu G, Zayzafoon M, Xu J, Shi C, Marshall FF, Zhou HE, Chung LW (2008) Receptor activator of NF-kappaB Ligand (RANKL) expression is associated with epithelial to mesenchymal transition in human prostate cancer cells. *Cell Res* 18: 858–870.
- Patrawala L, Calhoun-Davis T, Schneider-Broussard R, Tang DG (2007) Hierarchical organization of prostate cancer cells in xenograft tumors: The CD44 + {alpha}2{beta}1 + cell population is enriched in tumor-initiating cells. *Cancer Res* 67: 6796–6805.
- Patrikainen L, Porvari K, Kurkela R, Hirvikoski P, Soini Y, Vihko P (2007) Expression profiling of PC-3 cell line variants and comparison of MIC-1 transcript levels in benign and malignant prostate. *Eur J Clin Invest* 37: 126–133.
- Petrylak DP, Tangen CM, Hussain MH, Lara Jr. PN, Jones JA, Taplin ME, Burch PA, Berry D, Moynour C, Kohli M, Benson MC, Small EJ, Raghavan D, Crawford ED (2004) Docetaxel and estramustine compared with mitoxantrone and prednisone for advanced refractory prostate cancer. *N Engl J Med* 351: 1513–1520.
- Pettaway CA, Pathak S, Greene G, Ramirez E, Wilson MR, Killion JJ, Fidler IJ (1996) Selection of highly metastatic variants of different human prostatic carcinomas using orthotopic implantation in nude mice. *Clin Cancer Res* 2: 1627–1636.
- Qin J, Liu X, Laffin B, Chen X, Choy G, Jeter CR, Calhoun-Davis T, Li H, Palapattu GS, Pang S, Lin K, Huang J, Ivanov I, Li W, Suraneni MV, Tang DG (2012) The PSA(-/lo) prostate cancer cell population harbors self-renewing long-term tumor-propagating cells that resist castration. *Cell Stem Cell* 10: 556–569.
- Rajasekhar VK, Studer L, Gerald W, Socci ND, Scher HI (2011) Tumour-initiating stem-like cells in human prostate cancer exhibit increased NF-kappaB signalling. *Nat Commun* 2: 162.
- Selander KS, Brown DA, Sequeiros GB, Hunter M, Desmond R, Parpala T, Risteli J, Breit SN, Jukkola-Vuorinen A (2007) Serum macrophage inhibitory cytokine-1 concentrations correlate with the presence of prostate cancer bone metastases. *Cancer Epidemiol Biomarkers Prev* 16: 532–537.
- Senapati S, Rachagani S, Chaudhary K, Johansson SL, Singh RK, Batra SK (2010) Overexpression of macrophage inhibitory cytokine-1 induces metastasis of human prostate cancer cells through the FAK-RhoA signaling pathway. *Oncogene* 9: 1293–1302.
- Siegel R, Naishadham D, Jemal A (2012) Cancer statistics, 2012. *CA Cancer J Clin* 62: 10–29.
- Soto-Cerrato V, Vinals F, Lambert JR, Perez-Tomas R (2007) The anticancer agent prodigiosin induces p21WAF1/CIP1 expression via transforming growth factor-beta receptor pathway. *Biochem Pharmacol* 74: 1340–1349.
- Sun Y, Wang BE, Leong KG, Yue P, Li L, Jhunjunwala S, Chen D, Seo K, Modrusan Z, Gao WQ, Settleman J, Johnson L (2012) Androgen deprivation causes epithelial-mesenchymal transition in the prostate: implications for androgen-deprivation therapy. *Cancer Res* 72: 527–536.
- Tan M, Wang Y, Guan K, Sun Y (2000) PTGF-beta, a type beta transforming growth factor (TGF-beta) superfamily member, is a p53 target gene that inhibits tumor cell growth via TGF-beta signaling pathway. *Proc Natl Acad Sci USA* 97: 109–114.
- Tannock IF, de Wit R, Berry WR, Horti J, Pluzanska A, Chi KN, Oudard S, Theodore C, James ND, Turesson I, Rosenthal MA, Eisenberger MA (2004) Docetaxel plus prednisone or mitoxantrone plus prednisone for advanced prostate cancer. *N Engl J Med* 351: 1502–1512.
- Wakchoure S, Swain TM, Hentunen TA, Bauskin AR, Brown DA, Breit SN, Vuopala KS, Harris KW, Selander KS (2009) Expression of macrophage inhibitory cytokine-1 in prostate cancer bone metastases induces osteoclast activation and weight loss. *Prostate* 69: 652–661.
- Welsh JB, Sapinoso LM, Kern SG, Brown DA, Liu T, Bauskin AR, Ward RL, Hawkins NJ, Quinn DI, Russell PJ, Sutherland RL, Breit SN, Moskaluk CA, Frierson Jr. HF, Hampton GM (2003) Large-scale delineation of secreted protein biomarkers overexpressed in cancer tissue and serum. *Proc Natl Acad Sci USA* 100: 3410–3415.
- Wiklund FE, Bennet AM, Magnusson PK, Eriksson UK, Lindmark F, Wu L, Yaghouyfam N, Marquis CP, Stattin P, Pedersen NL, Adami HO, Gronberg H, Breit SN, Brown DA (2010) Macrophage inhibitory cytokine-1 (MIC-1/GDF15): a new marker of all-cause mortality. *Aging Cell* 9: 1057–1064.
- Wollmann W, Goodman ML, Bhat-Nakshatri P, Kishimoto H, Goulet Jr. RJ, Mehrotra S, Morimiya A, Badve S, Nakshatri H (2005) The macrophage

- inhibitory cytokine integrates AKT/PKB and MAP kinase signaling pathways in breast cancer cells. *Carcinogenesis* **26**: 900–907.
- Xu J, Kimball TR, Lorenz JN, Brown DA, Bauskin AR, Klevitsky R, Hewett TE, Breit SN, Molkentin JD (2006) GDF15/MIC-1 functions as a protective and antihypertrophic factor released from the myocardium in association with SMAD protein activation. *Circ Res* **98**: 342–350.
- Zhang L, Yang X, Pan HY, Zhou XJ, Li J, Chen WT, Zhong LP, Zhang ZY (2009) Expression of growth differentiation factor 15 is positively correlated with histopathological malignant grade and in vitro cell proliferation in oral squamous cell carcinoma. *Oral Oncol* **45**: 627–632.
- Zhao L, Lee BY, Brown DA, Molloy MP, Marx GM, Pavlakis N, Boyer MJ, Stockler MR, Kaplan W, Breit SN, Sutherland RL, Henshall SM, Horvath LG (2009) Identification of candidate biomarkers of therapeutic response to docetaxel by proteomic profiling. *Cancer Res* **69**: 7696–7703.
- Zheng Y, Xu Y, Ye B, Lei J, Weinstein MH, O'Leary MP, Richie JP, Mok SC, Liu BC (2003) Prostate carcinoma tissue proteomics for biomarker discovery. *Cancer* **98**: 2576–2582.

This work is published under the standard license to publish agreement. After 12 months the work will become freely available and the license terms will switch to a Creative Commons Attribution-NonCommercial-Share Alike 3.0 Unported License.

Supplementary Information accompanies the paper on British Journal of Cancer website (<http://www.nature.com/bjc>)